



Electrodeposition of ZnS Thin Films by Complexing Agent-Free Electrolyte Containing Sodium Thiosulfate as the Sulfur Precursor

H. M. L. U. Madhuwanthi¹ · G. D. K. Mahanama² · D. S. M. De Silva¹

Received: 21 November 2020 / Accepted: 9 April 2021 / Published online: 4 May 2021
© The Minerals, Metals & Materials Society 2021

Abstract

Thin films of zinc sulphide (ZnS) were prepared by a facile, economical, and scalable electrochemical method as a buffer layer for a CdS/CdTe based solar cell. Herein, a three-electrode cell in a complexing agent-free electrolyte containing 0.1 mol/L $\text{Na}_2\text{S}_2\text{O}_3$ and 0.1 mol/L ZnSO_4 was employed for the deposition of ZnS. The electrodeposition conditions (temperature: 30°C, pH: 4.2, cathodic potential: -1.10 V and deposition time: 90 min) were identified to grow an ideal thin film of ZnS on fluorine-doped tin oxide (FTO)-coated glass substrate, applying moderate stirring of 60 rpm. In material characterization of heat-treated samples (300°C, 10 min), the optical absorption measurement depicted a direct energy bandgap of 3.64 eV with low light absorbance and a blueshift from bulk ZnS. Scanning electron microscopy and atomic force microscopy studies demonstrated the uniform distribution of ZnS grains over the FTO glass substrate, and x-ray diffraction analysis revealed an amorphous structural nature of ZnS. The charge carrier density and flat-band potential of the ZnS material were determined as $1.19 \times 10^{-19} \text{ cm}^{-3}$ and -0.59 V, respectively, by Mott–Schottky analysis.

Keywords Buffer layer · complexing agent free · electrodeposition · sodium thiosulfate · zinc sulfide

Introduction

Zinc sulphide (ZnS) has been recognized as a II–VI semiconductor material due to its wide bandgap of (3.5–3.8) eV^{1–4} at room temperature, allowing the band to be tuned in the ultraviolet (UV) region. Also, it has a direct transition,⁵ high transparency,² and refractive index of 2.35,⁶ while it is non-toxic, cheap, and abundant.⁷ These properties make ZnS a potential candidate in applications such as decorative coatings, UV light-emitting diodes, field effect transistors, sensors, and buffer/window layers in photovoltaic solar cells.^{2,6,8,9} Pertaining to the photovoltaic solar cells, the wider bandgap and high transparency of ZnS thin films may effectively decrease the absorption losses in the window layer and increase the short-circuit current density of the cells.^{1,2,6,10} Therefore, ZnS may be considered a great replacement for cadmium sulphide (CdS) window material

in single-junction CdS/CdTe- and CdS/CuInGaSe₂-based solar cells.^{1,11–13}

Several techniques including chemical bath deposition (CBD), electrochemical atomic layer epitaxy (EC-ALE), molecular beam epitaxy (MBE), metal organic chemical vapor deposition (MOCVD), thermal evaporation, spray pyrolysis, successive ionic layer adsorption and reaction (SILAR), electrodeposition (ED), magnetron sputtering, and screen printing^{2,6,7,13–17} have been used to develop ZnS thin layers on different substrates. Physical techniques are expensive but more reliable, whereas the chemical techniques are cost-effective and scalable. Since the electrodeposition (ED) technique possesses the latter attributes,^{2,6,7,13,17} the focus herein is on an electrochemical study for developing thin films of ZnS by varying the electrolytic bath temperature, pH, and the deposition potential and time to control its electrical, optical, morphological and structural properties.

Reports of electrodeposition of ZnS thin layers without binding/complexing agents are scarce. Ammonia (NH_3), hydrazine (N_2H_4), trisodium citrate ($\text{Na}_3\text{C}_6\text{H}_5\text{O}_7$), glycerol ($\text{C}_3\text{H}_8\text{O}_3$), and ethylenediaminetetraacetic acid (EDTA) have often been used as complexing agents in the preparation of ZnS thin films.^{2,5,7,9,13,18} This report is based on a complexing agent-free cathodic electrodeposition technique

✉ D. S. M. De Silva
sujeewa@kln.ac.lk

¹ Department of Chemistry, University of Kelaniya, Kelaniya, Sri Lanka

² Department of Physics, University of Ruhuna, Matara, Sri Lanka

for developing ZnS thin films on fluorine-doped tin oxide (FTO)-coated soda lime glass substrates using sodium thiosulfate ($\text{Na}_2\text{S}_2\text{O}_3$) as the sulfur precursor for the electrodeposition of ZnS.

Materials and Methods

The electrodeposition processes were carried out using a potentiostat (GAMRY Series G300™) with a three-electrode cell consisting of a saturated calomel electrode (EDT DirectION, SCE), graphite rod (Sigma Aldrich, 99.995%) and glass/FTO substrate (Sigma Aldrich, $7\Omega/\text{sq.}$) as the reference, counter and working electrodes, respectively. The distance between the flat surface of the counter and working electrodes was maintained at 2 cm, while keeping both the reference and working electrodes in proximity. Prior to the experiments, the FTO substrates were cut into $3 \times 1 \text{ cm}^2$ pieces and cleaned by sonication in soap solution for 20 min, followed by rinsing in deionized water and then with acetone, methanol, and isopropanol, respectively.¹⁹ Cleaned FTO substrates were dried in hot air and stored in a desiccator.

The electrodeposition bath for ZnS consisted of 0.1 mol/L $\text{Na}_2\text{S}_2\text{O}_3$ and 0.1 mol/L ZnSO_4 . Both $\text{Na}_2\text{S}_2\text{O}_3$ and ZnSO_4 salts used were laboratory reagent grade from Sigma Aldrich. The ZnS thin films were electrodeposited on the FTO glass substrates by varying the temperature, pH of the bath, the deposition potential and time.

There are intercorrelations among the electrolyte conditions (concentration, temperature, and pH) in the occurrence of the chemical reaction in it. Hence, the experiments were designed first with a known concentration of constituent precursors (0.1 mol/L $\text{Na}_2\text{S}_2\text{O}_3$ and 0.1 mol/L ZnSO_4),

to identify the intercorrelation between the bath temperature and its pH. As S or S^{2-} formation by $\text{S}_2\text{O}_3^{2-}$ does not occur in a basic medium, the experimental pH range was initially narrowed to pH from 2.0 to 7.0. Thereafter, the visual appearance of a set of electrolytes at 30°C was studied with varying the pH from 2.0 to 7.0 in increments of 1.0 as shown in Fig. 1. Diluted H_2SO_4 and NH_4OH solutions were employed to adjust the solution pH.

When the bath used for the electrodeposition is precipitate-free, the undesirable extrinsic reactions and co-depositions may be negligible. Therefore, the purity of the target material would be high, and its electrical, optical, morphological and structural properties can be enhanced.¹⁹ According to Fig. 1, the electrolytes within a pH range of 4.0–5.0 at 30°C appeared precipitate-free, and hence pH 4.0 was initially selected to proceed to the next evaluations, and further pH adjustment will be discussed later.

In the process of identifying the workable temperature for electrodeposition of ZnS in the abovementioned electrolyte, temperatures above 30°C were found to be not viable due to turbid appearance (Fig. 2).

To determine the feasible deposition voltage range for ZnS, individual precursor solutions of 0.1 mol/L $\text{Na}_2\text{S}_2\text{O}_3$ and 0.1 mol/L ZnSO_4 and the corresponding electrolyte solutions were subjected to cyclic voltametric studies with forward and reverse cycles between 0 V and -2.00 V at a scanning rate of 0.05 V s^{-1} .

The standard reduction potential, E° , of Zn^{2+} and S^{2-} is -0.762 V and 0.449 V , respectively, with respect to the standard H_2 electrode. According to Fig. 3a, $\text{S}_2\text{O}_3^{2-}$ reduction starts at $\sim 0.60 \text{ V}$, while Zn^{2+} reduces (Fig. 3b) at $\sim 1.18 \text{ V}$. The voltammogram of the corresponding electrolyte solution (Fig. 3c) shows that the deposition of S and Zn starts at $\sim 0.65 \text{ V}$ and $\sim 1.13 \text{ V}$, respectively. Therefore, a cathodic

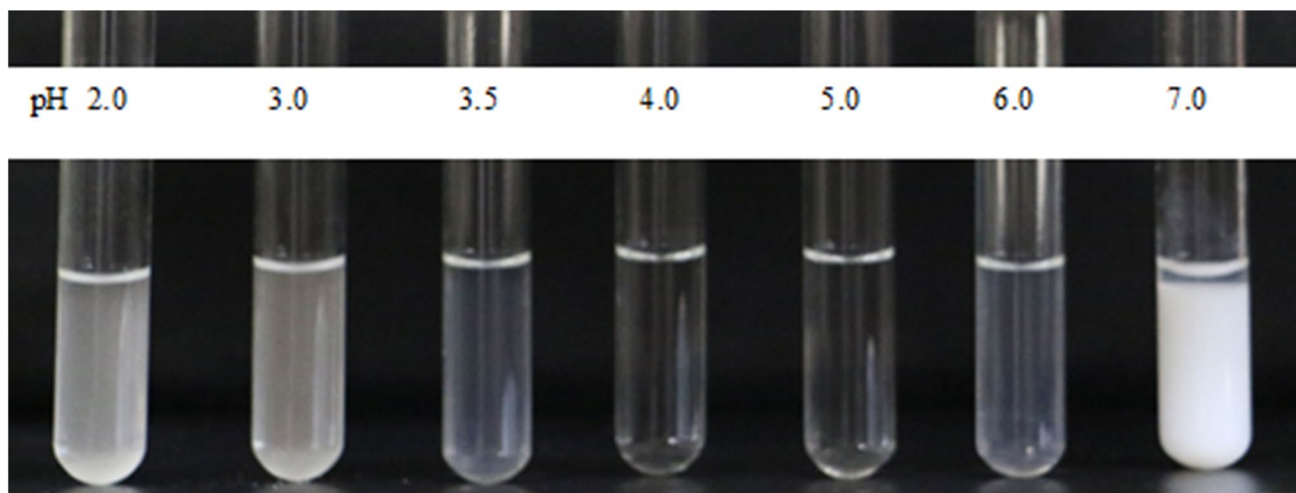


Fig. 1 The electrolyte solutions containing 0.1 mol/L $\text{Na}_2\text{S}_2\text{O}_3$ and 0.1 mol/L ZnSO_4 at pH of 2.0 to 7.0 and at 30°C .

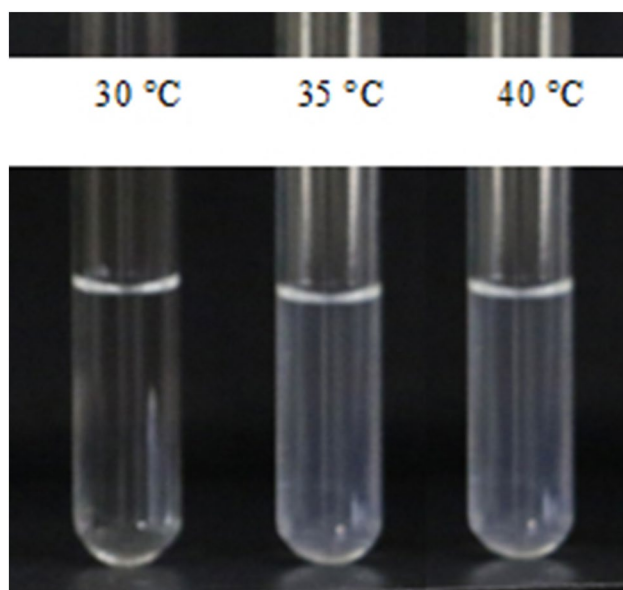


Fig. 2 The electrolyte consisting of 0.1 mol/L $\text{Na}_2\text{S}_2\text{O}_3$ and 0.1 mol/L ZnSO_4 at pH 4.0 and at temperatures of 30°C, 35°C, and 40°C.

potential range of -0.95 to -1.15 V was selected for further optimization.

Herein, electrodeposition of ZnS was performed under the above optimized pH (4.0) and temperature (30°C) applying -1.15 V potential with stirring of 60 rpm for 30, 45, 60, 75, 90, 105 and 120 min. A visually detectable film was formed in 90 min. Subsequently, selecting 90 min as the deposition time, ZnS samples were electrodeposited, varying the deposition potential, and their Tauc plots are compiled in Fig. 4. The Tauc plots, with no multiple peaks, aided in assuring the purity of the samples prepared. Optical absorption studies were performed using a UV/Vis spectrophotometer (Cintra 202 UV/Vis) after annealing the samples at 300°C for 10 min.

The ZnS thin film deposited at a cathodic potential of -1.10 V proved to be of the highest quality among the films prepared under given potentials, with a bandgap of ~ 3.6 eV. Hence, -1.10 V was selected as the ideal deposition potential for ZnS under the abovementioned deposition conditions. Next, the pH of the bath was subjected to further optimization standing at the abovementioned best deposition potential. Herein, several experiments were carried out within a pH range of 4.0 to 5.0 in increments of 0.1 at -1.10 V and 30°C. According to the resultant Tauc plots of the samples in Fig. 5, the sample prepared at pH 4.2 appeared to be free of undesirable extrinsic depositions and was hence selected as the optimal pH for this study.

Based on the above studies, the ideal deposition parameters for ZnS thin film formation on glass/FTO substrate in the electrolyte containing 0.1 mol/L $\text{Na}_2\text{S}_2\text{O}_3$ and 0.1 mol/L ZnSO_4 were a bath temperature of 30°C, pH 4.2, deposition

potential of -1.10 V, and deposition time of 90 min at a moderate stirring rate of 60 revolutions per min (rpm).

Scanning electron microscopy (SEM), atomic force microscopy (AFM), and X-ray diffraction (XRD) techniques were used to study the surface morphology and structural properties, and Mott–Schottky (MS) analysis was performed to determine the carrier density and flat-band potential of the ZnS thin films developed under the above conditions. The MS plots were measured in a typical three-electrode cell consisting of a saturated calomel electrode, graphite rod and the glass/FTO/ZnS substrate as the reference, counter and the working electrodes, respectively. A neutral 0.5 mol/L Na_2SO_4 was employed as the supporting electrolyte. The sinusoidal perturbation was 0.025 V with a frequency of 1000 Hz, with a linear scan from -0.60 to 0.40 V.

Results and Discussion

Structural Characterization

The XRD measurements were taken in the 2θ range of 20° – 80° using Cu $K\alpha$ radiation ($\lambda = 1.54060 \text{ \AA}$) for both glass/FTO and annealed glass/FTO/ZnS and shown in Fig. 6a and b. As there was no diffraction representing ZnS against the highly crystalline FTO substrate, the electrodeposited ZnS appeared amorphous. Similar observations were reported by Ojo, Salim, and Dharmadasa¹³ and Echendu and Dharmadasa¹² for ZnS thin films developed using $(\text{NH}_4)_2\text{S}_2\text{O}_3$ as the sulfur precursor in complexing agent-free electrolyte. Although the ZnS deposited in this study was structurally amorphous in nature, weak diffractions were observed (Fig. 6c) corresponding to competing phases of cubic (ZnS (200) C) and hexagonal (ZnS (002) H, ZnS (102) H).

The ZnS samples were deposited at a low temperature (30°C), and at this temperature, only the cubic phase can be anticipated, and the hexagonal phase tends to occur at elevated temperatures around 400°C.⁶ As the samples were annealed only at 300°C, the diffractogram predicts an induced transition from cubic to hexagonal with emerging diffractions by the planes (002), (200) and (102) as shown in Fig. 6c.

Surface Characterization

Figure 7 depicts the SEM image of the annealed (300°C, 10 min) ZnS thin layer grown at -1.10 V in the electrolyte consisting of 0.1 mol/L $\text{Na}_2\text{S}_2\text{O}_3$ and 0.1 mol/L ZnSO_4 at pH 4.2 and at 30°C for 90 min.

The grain sizes of the materials developed are influenced by the deposition potential, as below or above the optimum cathodic potentials the growth can be irregular due to

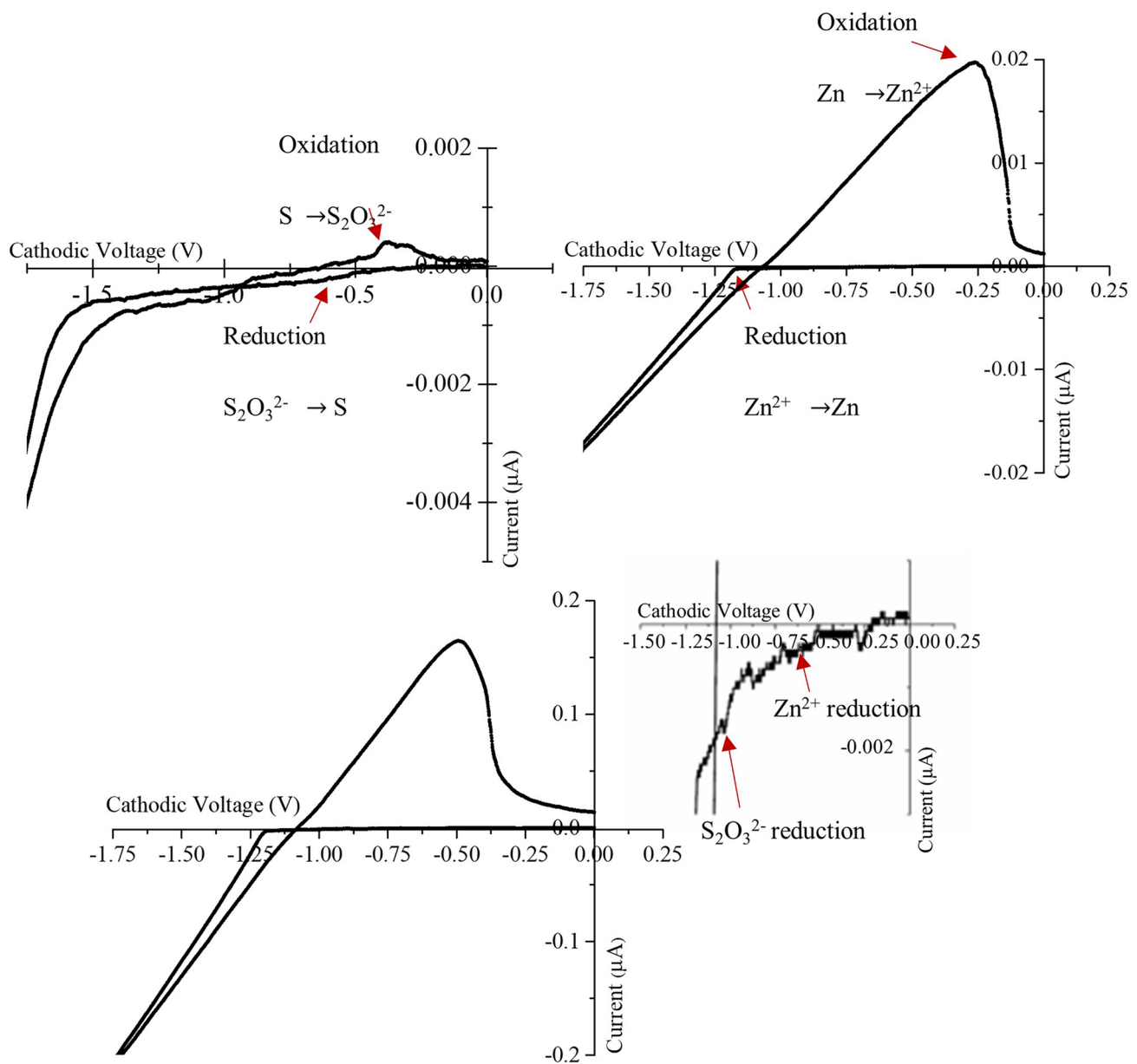


Fig. 3 Cyclic voltammograms for individual precursor solutions (a) 0.1 mol/L $\text{Na}_2\text{S}_2\text{O}_3$, (b) 0.1 mol/L ZnSO_4 and (c) electrolyte containing 0.1 mol/L $\text{Na}_2\text{S}_2\text{O}_3$ and 0.1 mol/L ZnSO_4 at pH 4.0 and 30°C .

incomplete growth of grains.⁷ The surface topology of the ZnS sample (Fig. 7) reveals the presence of nanoscale grains (242–448 nm) with sharp edges distributed uniformly on the FTO glass substrate. This uniformity is an indication of regular growth of grains under the optimized deposition conditions. The AFM study further evidenced the consistency of the nanograins over the substrate (Fig. 8) with surface roughness (root mean square roughness [rms]) of ~ 25 nm, which is much closer to that of glass/FTO (~ 26 nm).

Electrical Characterization

The flat-band potential and the charge carrier density can be estimated using Eq. 1.^{10,14}

$$\frac{1}{C^2} = \frac{2}{\epsilon\epsilon_0 e A^2 N_D} \left(E - E_{fb} - \frac{kT}{e} \right), \quad (1)$$

where C is the interfacial capacitance, ϵ is the dielectric constant ($\epsilon_{\text{ZnS}} = 8.1$), A is the electrode area exposed, ϵ_0 is the permittivity of free space (8.85×10^{-14} F/cm), k is the Boltzmann constant (1.38×10^{-23} J/K), N_D is the charge

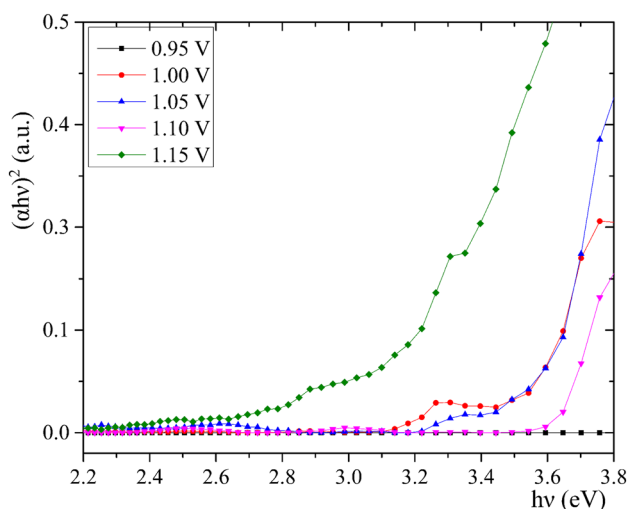


Fig. 4 The Tauc plot of ZnS thin films electrodeposited at cathodic potentials of -0.95 V to -1.15 V at 0.05 V intervals at pH 4.00 and at 30°C for 90 min.

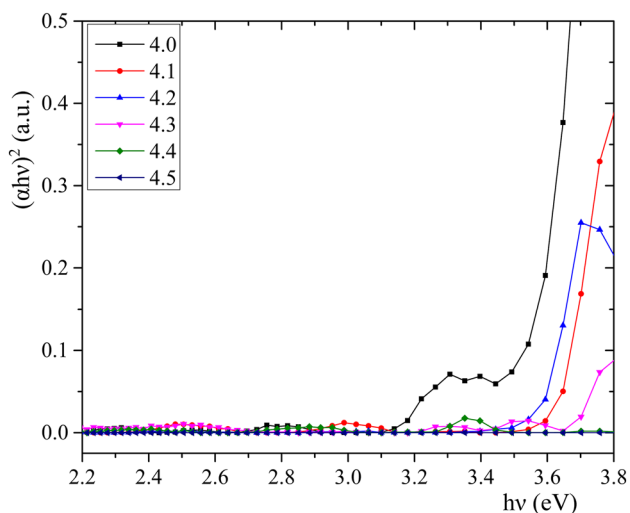


Fig. 5 Tauc plots of ZnS thin films electrodeposited at pH 4.0 to 4.5 in 0.1 intervals, at -1.10 V and at 30°C for 90 min.

carrier density, E is the applied potential, E_{fb} is the flat-band potential, T is the absolute temperature (298K), and e is the elementary charge of the electron (1.6021×10^{-19} C). The slope of the linear fit suggests the conductivity type of the sample, while the charge carrier density and flat-band potential can be calculated using the slope of the linear fit and the intersection of the linear fit with the potential axis, respectively.^{10,11,14,20}

The Mott–Schottky plot of the electrodeposited ZnS thin film is shown in Fig. 9. Accordingly, the positive slope of the linear plot confirmed the n -type conductivity, while the charge carrier density (N_D) and the flat-band potential

(E_{fb}) of ZnS were found to be $1.19 \times 10^{19} \text{ cm}^{-3}$ and -0.59 V, respectively.

Optical Characterization

The optical property evaluation of ZnS layers by UV-visible spectrophotometry in the 300 – 700 nm wavelength region revealed very low light absorbance by the sample in the visible region and the presence of a sharp absorption band edge at ~ 350 nm (Figs. 10 and 11), indicating the presence of a direct-bandgap material.¹ Therefore a thin layer of ZnS can effectively harness photons across both ultraviolet and visible regions and then transmit to the next layer. Such a feature is a vital characteristic of a buffer layer in a solar cell.

The bandgap deviation of a material from its theoretical value is an indication of impurities or defects present in the material.^{1,14,20}

$$\text{The Taucs formula is } \alpha = \frac{k(h\nu - E_g)^m}{h\nu},$$

where α is the absorption coefficient, E_g is the bandgap energy, h is Planck's constant, ν is the incident photon frequency and k is the proportionality constant. $m = 0.5$ for direct bandgap and $m = 2$ for indirect bandgap.

The bandgap of the deposited ZnS semiconductor material can be found using the graph of absorbance square (A^2) against photon energy ($h\nu$) by extrapolating the linear portion of the graph to the x-axis or using the Tauc plot of $(\alpha h\nu)^2$ against $(h\nu)$. The theoretical values were found to be ~ 3.6 eV and ~ 3.9 eV for cubic and hexagonal ZnS, respectively.¹³ According to the Tauc plot in Fig. 10, the bandgap of the electrodeposited ZnS under optimized conditions was 3.64 eV, while there were no multiple absorption edges here corresponding to impurity species, specially such as ZnO (3.37 eV) reported elsewhere.^{12,16} Further, the calculated bandgap of ZnS was blueshifted from bulk ZnS (3.50 eV),^{2,3} which can be attributed to the quantum confinement effect. It has been reported elsewhere that when the particle radius falls below the excitonic radius, the bandgap energy leads to a blueshift.^{16,21,22}

Conclusion

ZnS semiconductor thin films can be successfully electrodeposited on glass/FTO substrate using a three-electrode system consisting of a SCE, a graphite rod and a glass/FTO substrate as the reference, counter and working electrodes, respectively, in an electrolyte containing 0.1 mol/L $\text{Na}_2\text{S}_2\text{O}_3$ and 0.1 mol/L ZnSO_4 at a temperature of 30°C , pH of 4.2 , cathodic potential of -1.10 V and deposition time of 90 min, while stirring the bath at 60 rpm. The optical absorption

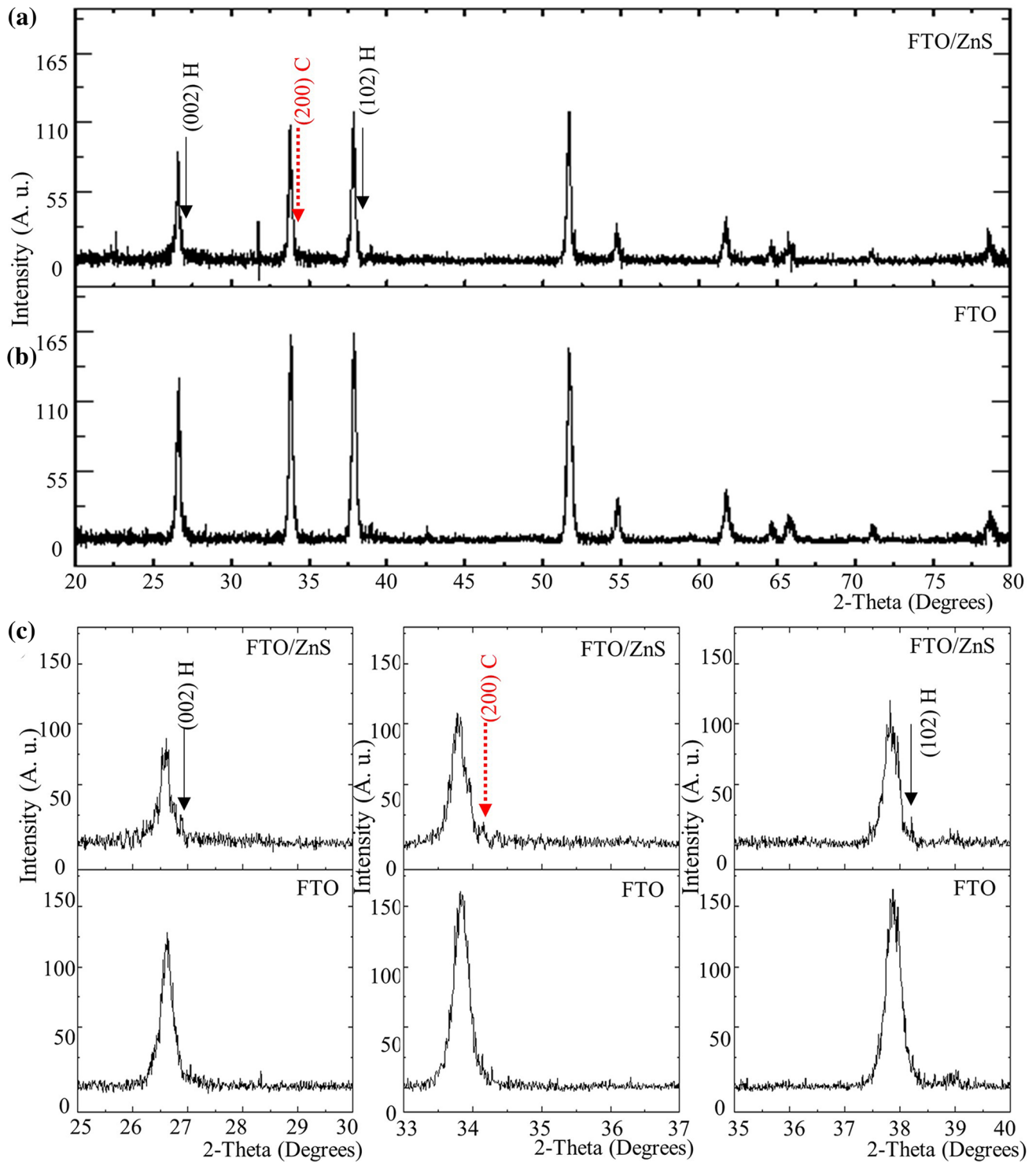


Fig. 6 The X-ray diffractograms of (a) annealed glass/FTO/ZnS, (b) glass/FTO and (c) expanded x-ray diffraction peaks along the (002), (200), and (102) planes.

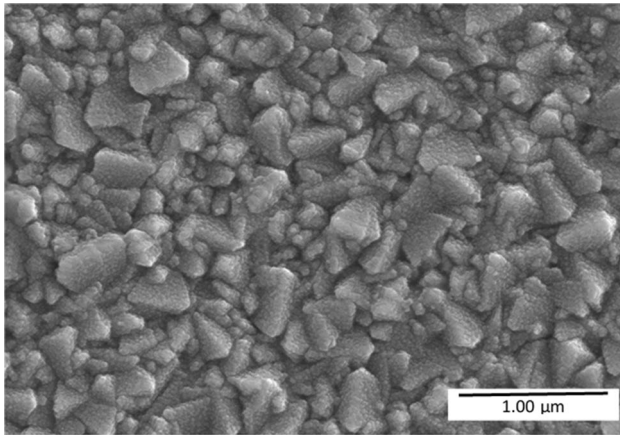


Fig. 7 SEM micrograph of annealed ZnS thin layer electrodeposited in the electrolyte containing 0.1 mol/L $\text{Na}_2\text{S}_2\text{O}_3$ and 0.1 mol/L ZnSO_4 at pH 4.2, -1.10 V and 30°C for 90 min.

measurement showed low light absorbance by the material, which is an ideal behavior of a buffer layer, while it has a direct energy bandgap of 3.64 eV, is free of co-deposited impurity species and shows a blueshift from bulk ZnS. The SEM and AFM studies demonstrated the uniform distribution of ZnS with 242–448 nm-sized grains and having sharp edges over the FTO glass substrate, with rms roughness ~ 25 nm. Further, XRD analysis revealed an amorphous ZnS structure, while competing phases of cubic and hexagonal ZnS peaks were observed with weak intensities. The ZnS material electrodeposited on the FTO substrate was revealed to be *n*-type in conductivity, with charge carrier density of $1.19 \times 10^{19} \text{ cm}^{-3}$ and flat-band potential of -0.59 V from the Mott–Schottky study.

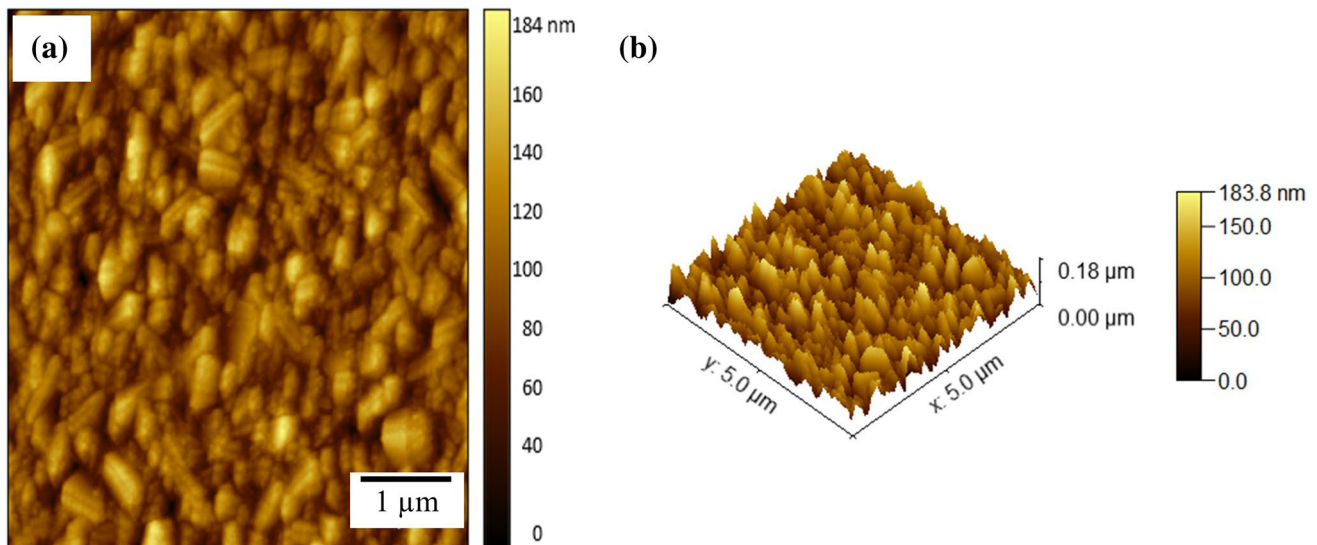


Fig. 8 (a) Two dimensional and (b) three-dimensional AFM images of annealed ZnS electrodeposited in the electrolyte containing 0.1 mol/L $\text{Na}_2\text{S}_2\text{O}_3$ and 0.1 mol/L ZnSO_4 at pH 4.2, -1.10 V and 30°C for 90 min.

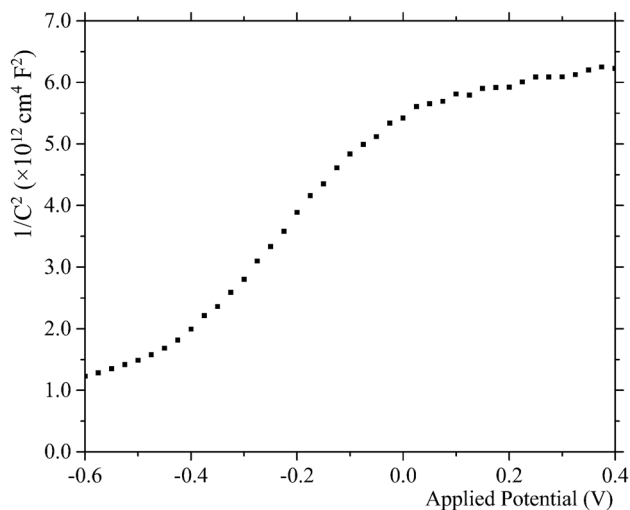


Fig. 9 Mott–Schottky plot of annealed ZnS electrodeposited in the electrolyte containing 0.1 mol/L $\text{Na}_2\text{S}_2\text{O}_3$ and 0.1 mol/L ZnSO_4 at pH 4.2, -1.10 V and 30°C for 90 min.

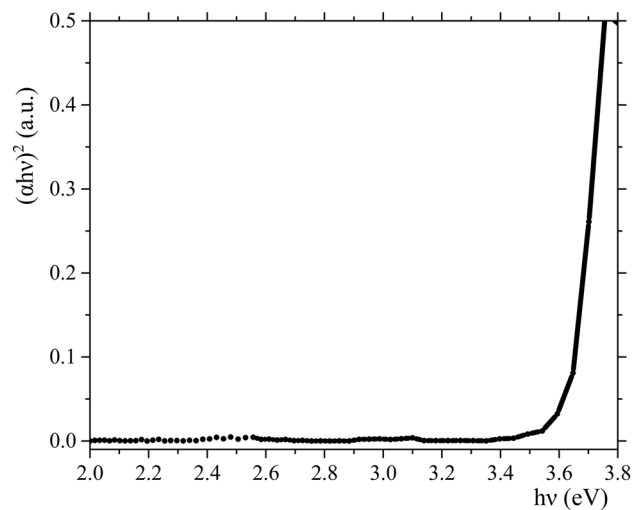


Fig. 11 The Tauc plot for the annealed ZnS layer electrodeposited in the electrolyte containing 0.1 mol/L $\text{Na}_2\text{S}_2\text{O}_3$ and 0.1 mol/L ZnSO_4 at pH 4.2, -1.10 V and 30°C for 90 min.

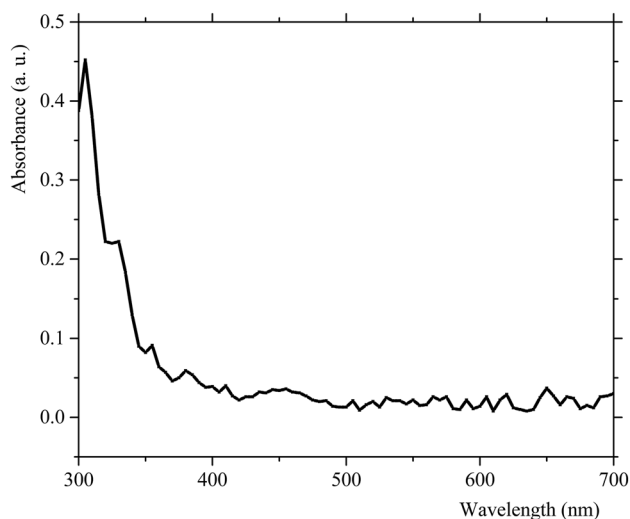


Fig. 10 The graph of absorbance against wavelength for the annealed ZnS layer electrodeposited in the electrolyte containing 0.1 mol/L $\text{Na}_2\text{S}_2\text{O}_3$ and 0.1 mol/L ZnSO_4 at pH 4.2, -1.10 V and 30°C for 90 min.

Acknowledgments Financial assistance of the State Ministry of Skills Development, Vocational Education, Research and Innovation, Sri Lanka, under the Edu-Training program on Prototype Manufacturing of Solar Panels and the NSF equipment grant (RG/2013/EQ/02) are acknowledged.

Conflict of interest The authors declare that they have no known competing financial interests or personal relationships that could have appeared to influence the work reported in this paper.

References

1. M.H. Doha, M.J. Alam, J. Rabeya, K.A.M.H. Siddiquee, S. Husain, O. Islam, M.A. Gafur, S. Islam, N. Khatun, and S.H. Sarkar, *Optik (Stuttg)*. 126, 5194 (2015).
2. M. Izi, G. Heidari, S.M. Mousavi Khoie, and J. Najafi, *Surf. Eng. Appl. Electrochem.* 53, 245 (2017).
3. R. John, and S. Florence, *Chalcogenide Lett.* 7, 269 (2010).
4. H. Zhu, J.F. Huang, Y. Wang, L.Y. Cao, H.Y. He, and J.P. Wu, *Surf. Eng.* 27, 42 (2011).
5. A.B. Bhalerao, C.D. Lokhande, and B.G. Wagh, *IEEE Trans. Nanotechnol.* 12, 996 (2013).
6. F. Zakerian, and H. Kafashan, *Superlattices Microstruct.* 124, 92 (2018).
7. A. Kassim, S. Nagalingam, H.S. Min, and N. Karrim, *Arab. J. Chem.* 3, 243 (2010).
8. T. Öznüller, I. Erdogan, and Ü. Demir, *Langmuir* 22, 4415 (2006).
9. X. Xu, F. Wang, Z. Li, J. Liu, J. Ji, and J. Chen, *Electrochim. Acta* 87, 511 (2013).
10. B. Long, S. Cheng, H. Zhou, J. Liao, H. Zhang, H. Jia, and H. Li, *ECS Solid State Lett.* 3, 140 (2014).
11. A.A. Ojo, and I.M. Dharmadasa, *Sol. Energy* 158, 721 (2017).
12. O.K. Echendu, and I.M. Dharmadasa, *Energies* 8, 4416 (2015).
13. A.A. Ojo, H.I. Salim, and I.M. Dharmadasa, *J. Mater. Sci. Mater. Electron.* 29, 13631 (2018).
14. K. Ghezali, L. Mentar, B. Boudine, and A. Azizi, *J. Electroanal. Chem.* 794, 212 (2017).
15. M.L. Madugu, O.I.O. Olusola, O.K. Echendu, B. Kadem, and I.M. Dharmadasa, *J. Electron. Mater.* 45, 2710 (2016).
16. O.K. Echendu, A.R. Weerasinghe, D.G. Diso, F. Fauzi, and I.M. Dharmadasa, *J. Electron. Mater.* 42, 692 (2013).
17. A. Kassim, H.S. Min, A.H. Abdullah, N. Karrim, and S. Nagalingam, *Dig. J. Nanomater. Biostructures* 5, 975 (2010).
18. A. A. Ojo, W. M. Cranton, and I. M. Dharmadasa, Next Generation Multilayer Graded Bandgap Solar Cells (2019).
19. H.Y.R. Atapattu, D.S.M. De Silva, K.A.S. Pathiratne, O.I. Olusola, and I.M. Dharmadasa, *J. Mater. Sci. Mater. Electron.* 28, 18592 (2017).
20. A. Azmand, and H. Kafashan, *Ceram. Int.* 44, 17124 (2018).

21. Y. Li, Y. Ding, Y. Zhang, and Y. Qian, *J. Phys. Chem. Solids* 60, 13 (1999).
22. K.S. Rathore, D. Patidar, Y. Janu, N.S. Saxena, K. Sharma, and T.P. Sharma, *Chalcogenide Lett.* 5, 105 (2008).

Publisher's Note Springer Nature remains neutral with regard to jurisdictional claims in published maps and institutional affiliations.